Molecular Crystals and Liquid Crystals
Publication details, including instructions for authors and subscription information:
http://www.tandfonline.com/loi/gmcl20

Surface-Polymer Stabilized Liquid Crystals

Jean-Philippe Bédard-arcand [a] & Tigran Galstian [a]
[a] Center for Optics, Photonics and Laser, Department of Physics, Engineering Physics and Optics, Laval University, Pav. d'Optique-Photonique, 2375 Rue de la Terrasse, Québec, Canada, G1V 0A6
Version of record first published: 15 May 2012.

To cite this article: Jean-Philippe Bédard-arcand & Tigran Galstian (2012): Surface-Polymer Stabilized Liquid Crystals, Molecular Crystals and Liquid Crystals, 560:1, 170-182

To link to this article: http://dx.doi.org/10.1080/15421406.2012.663520

Mol. Cryst. Liq. Cryst., Vol. 560: pp. 170–182, 2012

ISSN: 1542-1406 print/1563-5287 online
DOI: 10.1080/15421406.2012.663520

Taylor & Francis
Taylor & Francis Group

Surface-Polymer Stabilized Liquid Crystals

JEAN-PHILIPPE BÉDARD-ARCAND
AND TIGRAN GALSTIAN*

Center for Optics, Photonics and Laser, Department of Physics, Engineering Physics and Optics, Laval University, Pav. d'Optique-Photonique ,2375 Rue de la Terrasse, Québec, Canada G1V 0A6

We report the creation and study of an electrically controllable self-organized surface-polymer stabilized liquid crystal system. We use thin reactive mesogen films as alignment layers to build cells filled by a pure non-reactive nematic liquid crystal (LC). The application of external fields during the photo polymerization of the reactive mesogen layer allows us the control of scattering properties of obtained cells. We investigate the system's morphology and optical behaviour by using electro optical scattering and microscopy to show that the use of this approach enables very interesting performance compared to traditional "bulk" LC-based composite light shutters.

Keywords Amplitude modulator; light scattering; liquid crystal polymer composite; reactive mesogens; surface stabilized alignment

Introduction

Bulk (or volume) polymer dispersed and polymer stabilized LC composites (respectively called PDLC [1–3] and PSLC [4,5]) are promising for cost-effective light modulation applications (displays, optical shutters, smart windows). However their short term stability (e.g., the aggregation or deterioration of mixed reactive constituents during the manufacturing, etc) as well as long term stability (such as yellowing, etc.) are rather problematic.

In the present work, we use a different approach for controlling the morphology and electro-optical properties of LC cells. Namely, the polymer network (e.g., made from a Reactive Mesogen/RM) here is "attached" to the surface of the substrate instead of being dispersed in the volume of the cell; that is why we further name it as S-PSLC (see also [6–8]). In addition, our approach is based on the use of electric and/or magnetic torques (see later) to first align the pure LC (in the bulk of the cell) as well as the surface-cast RM molecules in their liquid crystalline (nematic) phase and then the use of the reactivity of RM molecules to polymerize them by using UV light exposition. The obtained permanent surface-attached polymer network then defines the orientational morphology of the cell and its electrooptic behaviour.

We have already reported some preliminary results of this approach, describing the experimental observation of UV light induced self-organization of 2D periodic structures

*Address correspondence to Tigran Galstian, Center for Optics, Photonics and Laser, Department of Physics, Engineering Physics and Optics, Laval University, Pav. d'Optique-Photonique, 2375 Rue de la Terrasse, Québec, Canada G1V 0A6. Phone 418 656 2025. E-mail: galstian@phy.ulaval.ca

at the interface of nematic LC and RM layers [9]. In the present work, we report the results of our electrooptical and microscopy studies performed on those S-PSLC systems.

Materials and Methods

The S-PSLC cell was built by using two commercial glass substrates covered by transparent conductive indium tin oxide (ITO) coatings. Two additional layers were coated on the ITO surfaces prior to the LC cell construction. The first one was a standard alignment layer of Polyimide (PI-150, from Nissan). The second one was a layer of RM (RMS03-001C, from Merck) of positive anisotropy ($n_o = 1.525$, $\Delta n = 0.155$) typically used for "planar alignment" layers [10]. The cell was filled with a standard (non-reactive) nematic LC (TL216, from Merck) of positive anisotropy ($n_o = 1.5237$, $\Delta n = 0.2112$). The cell's interior structure was hence formed by two thin layers of RM (facing each other) sandwiching a bulk non-reactive LC, see Fig. 1.

In more details, the PI-150 was spin-coated on the ITO-glass substrate (following the instructions from Nissan; 3000 rpm for 30 sec), heated (at 280°C) and rubbed to obtain an alignment layer of ≈50 nm thick. The RM was afterward spin-coated (3000 rpm for 30 sec) onto the rubbed PI-150 layer to obtain a ≈ 600 nm thick RM film. The obtained substrate was then dried and annealed by heating for 300 sec at 60°C on a temperature controlled hot-stage. Before the RM layer is polymerized by UV light (as it should normally be done as a next step), the LC cell was built by drop fill method : the first substrate was placed horizontally with the RM layer facing up, the LC was spread onto the RM layer, then a similar substrate was pressed on the LC with its RM layer facing down. The final (peripheral only) sealing of the cell was done by using a UV curable resin which was spread on the periphery of the first substrate. This resin contained glass spacers of diameter Ø ≈ 50 ± 2 μm to provide the desired thickness of the cell.

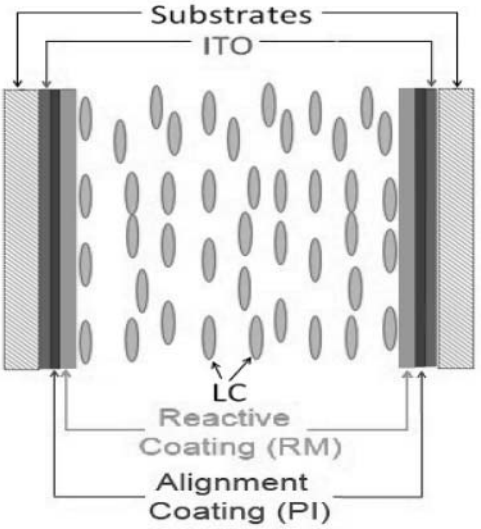

Figure 1. Side-view schematic representation of the S-PSLC cell.

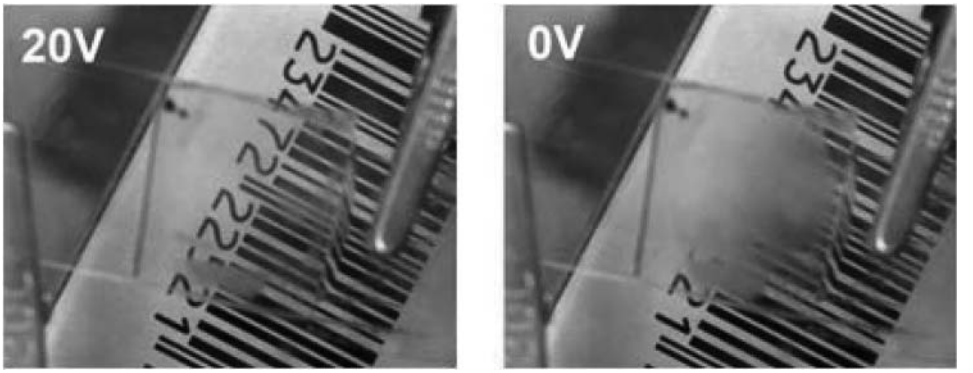

Figure 2. Qualitative demonstration of the cell's scattering in its ground state (right picture, U = 0 V) and when subjected to 20 V RMS voltage (left picture). The photo is made in polarized light, the polarizer's transmission axis being aligned in the rubbing direction of the PI-150.

The LC cell was then subjected to electric field during a certain period of time (the RM layers still being in their nematic phase). This allowed reorientation and some partial interpenetration of LC and uncured RM molecules, prior to the total curing of RM (by using UV light with spectra between 300 nm–450 nm, intensity of $\approx$10 mW/cm^2, irradiation time $\leq$10 min, exposition at room temperature T = 22°C, with particular attention to avoid heating). We have optimized several experimental parameters, such as the pre-exposition time (partial gelification of RM before the cell construction and field application), the 'dark' polymerization time (between the end of the partial UV polymerization and the beginning of the contact with LC), the time of inter diffusion between RM and LCs, etc. As an example of a particular set of parameters, we present here the case of: 5–10 minutes of inter diffusion, 0–1 minute of partial polymerization (pre-exposition), 5–10 minutes of 'dark' polymerisation and applied "programming" electrical fields (during the UV curing) in the range from 20 V to 110 V. The obtained cells were subjected to a critical voltage pulse (again in the range from 20 V to 110 V) and were then stabilized in their scattering ground-state. A macroscopic view of the obtained cell (for two values of applied voltage) is presented in the Fig. 2. We can see that the cell becomes transparent (clear) already at U = 20 V of control voltage (AC of SIN form at 1 kHz).

The obtained cells were then subjected to electro-optical angular scattering measurements, the general scheme of the experimental set-up being schematically presented in the Fig. 3.

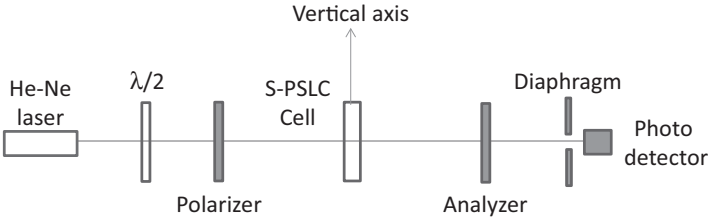

Figure 3. Schematics of the general experimental setup used for the "programming" and for the electro-optical study of the haze and angular light scattering of S-PSLC cells.

CW He-Ne laser beam (operating at 632.8 nm) was used as probe. Two Glan prisms were used as polarizer and analyzer. A half-wave plate ($\lambda/2$) was used to set the power of the probe beam, incident on the cell. The second Glan prism (analyzer) was used only for real-time acquisition during the initial "programming" (see later) stage of the experiments. LabView system and a driving voltage generator were used for data acquisition and cell control. The diameter of the diaphragm (positioned just in front of the photo detector) was 1 mm and its distance from the sample was chosen in a way to have a collection angle of 0.5°. The couple of the diaphragm and detector was swept angularly (staying in the horizontal plane) to detect the angular distribution of scattered light power. Haze experiments were performed by using the same set-up, but by rotating the sample (around the vertical axis passing by the probe light's incidence point, see Fig. 3) with however only the input polarizer being in place (the analyzer was removed in all experiments after being used for "programming" only).

A last note should be made on the technique employed for surface analysis. As a first step we have constructed the cell and performed our electro optical tests. Afterwards we separated both substrates taking particular care to keep the internal surfaces of the cell unaffected. Then we dissolved the remaining on the surface LC molecules by the solvent (isopropanol), evaporated and dried the substrate in the vacuum. This last step ensures that there is no residual LC encapsulated and that the substrate will be insensitive to later performed surface analysis.

Electro-Optic Study

The reorientation of the director ***n*** (average direction of long molecular axes of the LC [11,12]) of the cell was monitored (by the variations of the electric field-induced phase retardation thanks to the polarimetric set-up, Fig. 3) from the moment when the "programming" electric field was applied, through the start of the UV curing and until the polymerisation of the RM was as close as possible to 100% (experimentally determined curing duration, see later). In this way, we ensured that the director was reoriented before the UV curing of the RM. As the curing was done, we have removed the field. As already mentioned above, the obtained final cells were scattering in their ground state (Fig. 2, right picture) after a short-period exposure to high voltage for morphology "stabilization".

We started our characterization by studying the steady state ballistic transmission of the probe light (at normal incidence) through the cell upon the applied voltage (the diaphragm and detector are directly facing the incident light, at 0° angle). The polarization of the incident probe was set to be parallel to the rubbing direction of the PI-150. The corresponding results are presented in the Fig. 4. As one can see, the transmission increases with the increase of applied voltage. The final (maximal) transmission of the probe beam was estimated to be $\approx$100% (taking into account the Fresnel reflections from the cell substrates and from ITO coatings as well as the ITO absorption). The contrast ratio, obtained for an excitation level of 2 V/μm, is equal to $9.986/0.075 \approx 133$.

The inset of the Fig. 4 shows a zoom on the low-voltage zone where we can see that the transmission increases after the voltage is above a quasi-threshold.

The polarization dependence of scattering for the obtained element was measured in a separate experiment. The light transmission was first measured at U = 110 V (clear state) and then the applied voltage was decreased quickly (from 110 V to 0 V) for two cases; when, first, the input probe's polarization was parallel, and then perpendicular to the rubbing direction of PI-150. The Fig. 5 shows the typical transmissions obtained with those two polarizations. The used S-PSLC cell was fabricated (UV cured) in the presence of a

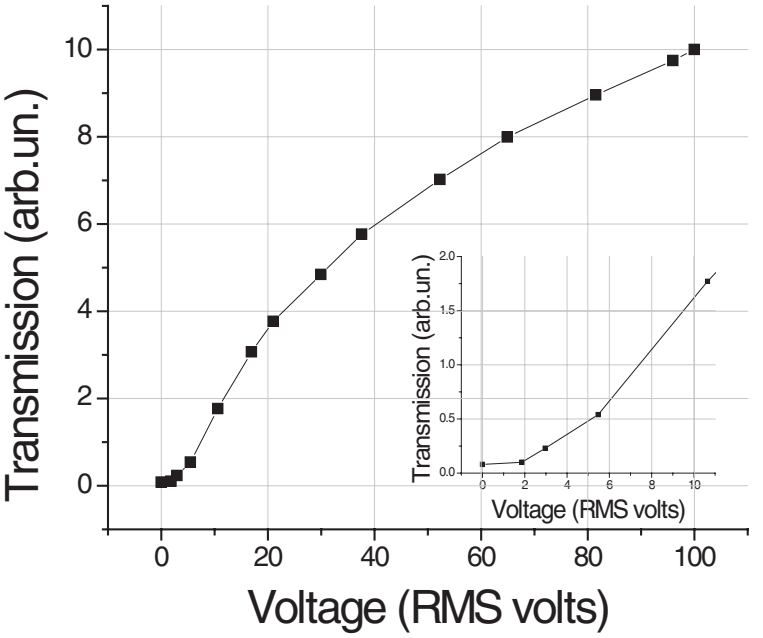

Figure 4. Steady state transmission dependence upon the RMS voltage for the cell of S-PSLC that was UV cured in the presence of an electric field of 20 V; incident probe's polarisation is parallel to the rubbing direction. The experimental error here is estimated to be ≈5%.

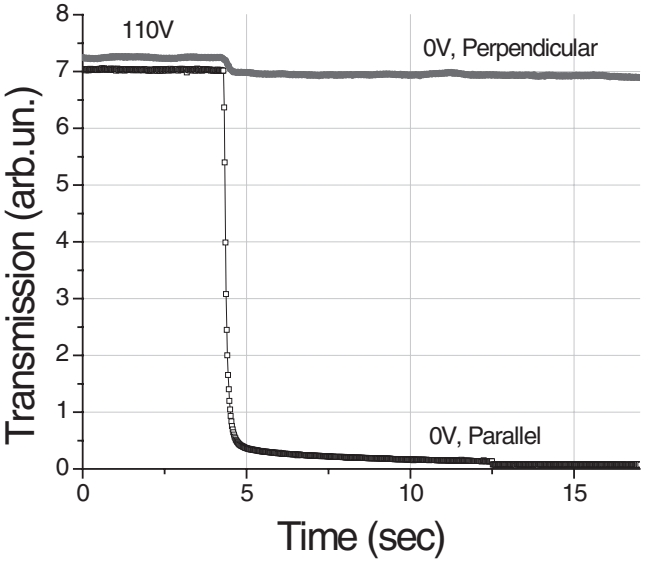

Figure 5. Polarization dependence of light transmission through the S-PSLC cell (ballistic transmission). A voltage of U = 110 V is applied to the cell initially. This voltage is then switched off (U = 0 V) at approximately t = 4 sec.

50 V "programming" electric voltage. As one can see, there is a very strong anisotropy of scattering. The modulation contrast (ratio of transmission with and without voltage) for the extraordinary polarization of the probe is very high (≈142); while it is only ≈1.06 for the ordinary polarization of the probe.

The established ratio of ground state transmission coefficients for parallel and perpendicular polarizations of the probe is equal to 6.9/0.05 ≈140. Note, as a reference, that the detected transmission value was "equal" to ≈9 without the cell being on the optical path of the probe beam (and without analyzer). Thus, the residual scattering may be estimated to be very low (≈1%; the transmission loss from the ITO coated substrate was ≈9 – 10%).

The next step of characterization of the cell was done to study the transition times as well as the stability of its operation. This was done by multiple cycles of nematic-isotropic phase transitions (by heating and cooling the cell) and by rapid on-off switches of the applied voltage in the nematic phase of the cell. The S-PSLC cell was fabricated (UV cured) in the presence of a 50 V "programming" electric voltage. The polarization of the input probe beam was parallel to the rubbing direction of the PI-150. The obtained results are shown in the Fig. 6 for off-on cycles using voltage switches from 20 V to 0 V.

The high transmission state here corresponds to the voltage U = 20 V applied to the cell; while the voltage is removed (U = 0 V) for the low transmission state. The contrast of the scattering first increases (with switching cycles) and then stabilizes at ≈125.

Then, the angular scattering of our cells was characterized by rotating the couple of diaphragm and detector (both staying in the horizontal plane) around the S-PSLC cell. The S-PSLC cell was fabricated (cured) in the presence of a 50 V "programming" electric voltage. The polarization of the input probe beam was parallel to the rubbing direction of the PI-150. This was done to complement our ballistic measurement studies. The corresponding dependence of the scattered power upon the scattering angle is shown in the Fig. 7. Just for an example, with those measurements, we have calculated the contrast ratio for ballistic (at 0° angle) and slightly angularly tilted (at ≈0.5° angle) transmissions and obtained

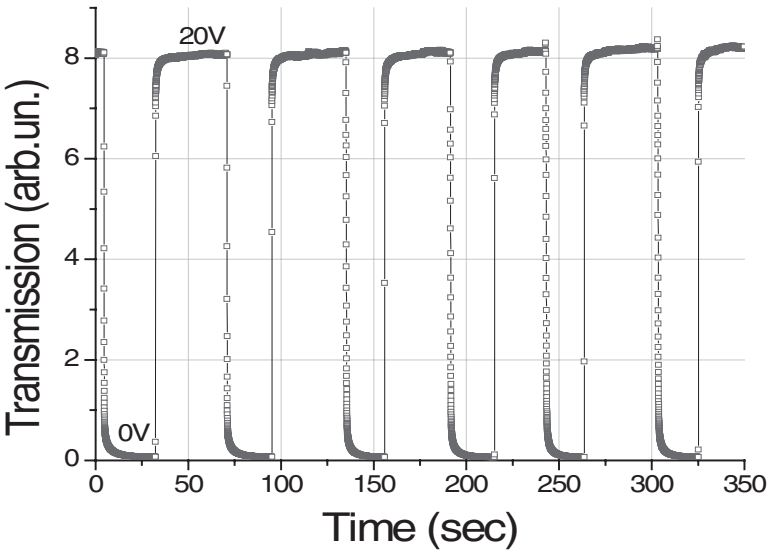

Figure 6. Electro-optic stability and transition speed tests of the cell of S-PSLC. The transmission values are measured for two states, U = 20 V (high transmission) and U = 0 V (low transmission).

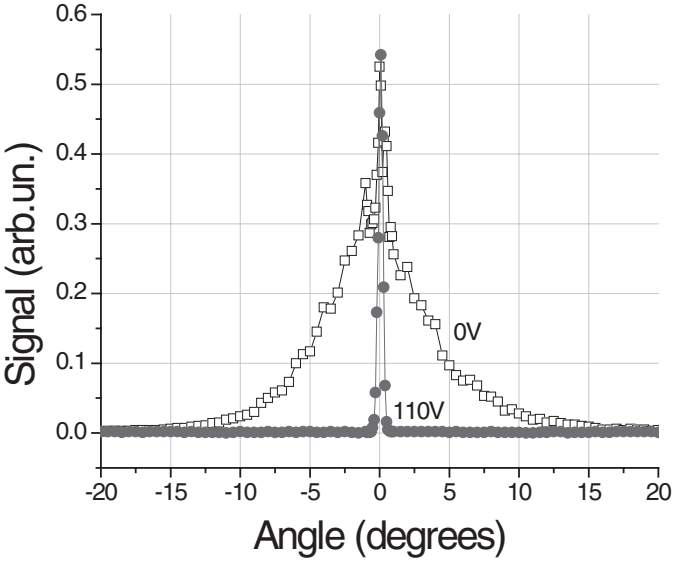

Figure 7. Electro-optic study of the angular scattering of the S-PSLC cell (normalized to the maximal value of the ground state's ballistic transmission by reducing that value in the clear state by a factor of 433).

contrast rations (between the scattering and clear states of the cell) ∼450 and ∼100, respectively.

Finally, the angular haze of our cells was measured by keeping the diaphragm and detector facing directly the probe beam (at 0° angle), while rotating the cell around the vertical axis (the rubbing direction of the PI-150 being kept in the horizontal plane). In this way, the incidence angle of the probe beam was changed gradually in both directions. The polarization of the probe beam was set to horizontal (thus, being parallel to the rubbing direction in the case of normal incidence of the probe). The incidence point of the probe was kept the same during this rotation. The same measurements were made in the presence of an electric voltage (U = 110 V) and in its absence (U = 0 V). As we can see, (Fig. 8, open squares) the transmission of the cell is very low and relatively angle-independent in its ground state (U = 0 V). The application of the field increases the transmission of the probe (Fig. 8, filled circles). Here also, the angular dependence is rather "soft" compared to typical PDLCs [13]).

Discussion of Electro-Optic Results

It is clear that the applied fabrication process generates a network of polymer, which perturbs the alignment of the LC in its ground state. Those defects of alignment have very specific character. First, they may be temporarily homogenized by the application of relatively weak electric fields (Fig. 4). This homogenization takes place above a quasi-threshold (≈2 V). It is worthy to note that the director reorientation threshold in the pure LC should be at the same order of magnitude (≈1.76 V). This value was estimated by using the well-known formula [12])

$$V_{Thresh} \approx \pi \sqrt{K_1/(\varepsilon_0 |\Delta\varepsilon|)} \quad (1)$$

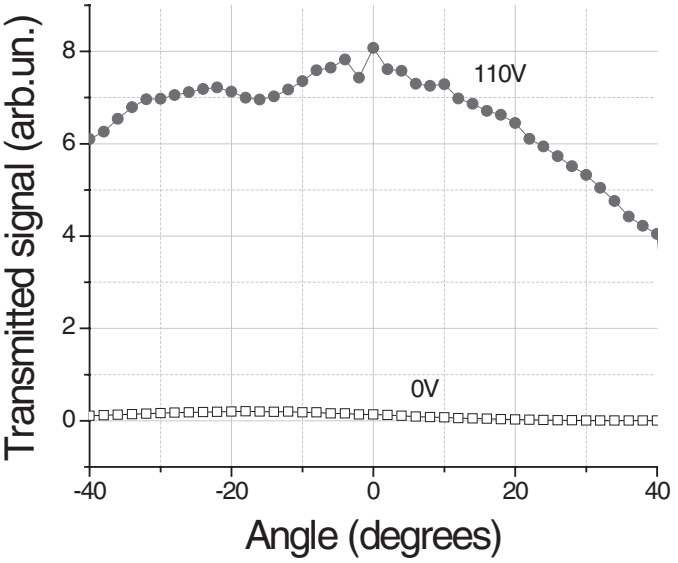

Figure 8. S-PSLC cell's angular haze; probe transmission versus incidence angle for two voltage values; filled circles show the high transmission state (for U = 110 V) and the open squares show the strongly scattering state with (U = 0 V).

and material parameters of the LC used (the elastic constant $K_1 \approx 15.3$ pN and dielectric anisotropy $\Delta\varepsilon = 5.5$, [10]). This indicates that the reorientation of the director is initiated in the bulk (as in standard cells) and then it is propagated to the near-surface zones, which are responsible for director non-uniformities and corresponding light scattering (their homogenization results in the increase of transmission).

Second, the director defects are aligned in their ground state, since the observed light scattering is strongly anisotropic (by a factor of ≈140, Fig. 5). Given that the scattering cross section (in LCs) is usually proportional to the Δn^2 (where $\Delta n \equiv n_{\parallel} - n_{\perp}$ is the optical birefringence of the LC, in this case $\Delta n = 1.7349–1.5237 = 0.2112$), this would mean that the local anisotropy perturbations, which are believed to be in the origin of light scattering, are at least 10 times more important in the plane σ, composed by the director and the electric field, compared to those in the perpendicular direction (out of σ). This being said, we should remember that the initial ellipsoid of indexes is aligned in the rubbing direction and, consequently, it would take rather important angles of out of σ reorientation to generate comparable optical perturbations for the ordinary polarized probe beam. As an example, one degree tilt of the director (with 3° of pretilt) out of σ would generate ≈1.7 times stronger variation of the effective refractive index for the extraordinary mode compared to the ordinary mode of probe polarization (see also Ref. [14]).

Furthermore, the multiple thermal and electrical cycling of cells (see Fig. 6) shows that the obtained morphology is stable (obviously, separate reliability tests should be done to complete this study). The scattering modulation speed was fit by a bi-exponential formula: $S = S_0 + A_1 \exp(-(x - x_o)/t_1) + A_2 \exp(-(x - x_o)/t_2)$. The obtained results show that, initially, the obtained cells show relatively complex and slow relaxation (3–4 sec), but, after multiple cycles, the main contribution may be described as mono exponential and the corresponding relaxation time (of the re-establishment of *scattering*) may be described as $t_1 \approx 0.315 \pm 0.005$ sec. Interestingly enough, the characteristic relaxation time for a $L = 50\ \mu$m thick uniform cell may be estimated to be ≈4.92 sec, by using the following formula

and parameters (see, e.g., Ref. [15])

$$\tau_R \approx \gamma L^2/(K_1\pi^2) \tag{2}$$

where γ is the rotational viscosity of the LC ($\gamma = 297$ mPa s or 0.297 s N/m^2 at 20°C). This shows again that, at the initial stages, the director non-uniformity size is comparable with the cell's size, but after its "stabilization", the characteristic sizes of defects, responsible for scattering, must be at the order of ≈ 4 μm (since the relaxation time is defined by the square of the effective cavity length).

The corresponding excitation time (of reduction of *scattering*) may also be analyzed theoretically. Thus, the typically measured excitation time of S-PSLC cells was estimated to be $t_{excit} \approx 0.034 \pm 0.008$ sec. This is rather close to the theoretical value of excitation in the pure LC cell (≈ 0.038 sec), taking into account the threshold of reorientation and the formula

$$\tau_{ON} \approx \tau_R/[(V/V_{Thresh})^2 - 1] \tag{3}$$

The LC scattering is well known to have a large angular distribution due to the dynamic fluctuations of the director [11]. Figure 7 shows that the obtained cells may be used to control that distribution rather efficiently. Thus, in a very rough approximation, the experimentally observed angular distribution of light power was fit by using the following Gaussian distribution formula $S = S_0 + A \exp(-0.5((x - x_c)/w)^{2)}$, which yield an increase of full width at half maximum by a factor of 7.46°(scattering state)/0.39° (transparent state) ≈20.

Finally, the haze measurements show (Fig. 8) that the incidence angle dependence of scattering (still for the extraordinary input polarization) is rather uniform, remaining above 75% at least for the range of incidence angles ±20°. Note that the transmission coefficient for the incidence angle of 20° is ≈90% for the parallel polarization added to the total substrate loss of ≈20%.

Surface Morphology Study

We have then proceeded to the study of the morphology of the substrate by using a Scanning Electron Microscope (model Quanta 3D FEG). The preparation procedure of those substrates was already described above. As we can see (from the Fig. 9), two specific morphological signatures are visible on the surface of obtained substrates (from the washed S-PSLC cells). The first one is the presence of relatively short (ranging from 3 μm to 30 μm), narrow (at the order of 1 μm) and well aligned (in the rubbing direction; here "from left to right") polymer "fiber bundles". The second feature is the presence of much larger polymer aggregates (again on the surface, but in form of elongated or star-shaped "islands"), which have rather chaotic alignments and almost no correlation with the previous (aligned) polymer structure. The length and width of those large aggregations range, respectively, from 20 μm to 50 μm and from 3 μm to 7 μm. Both the horizontally aligned and chaotically distributed (larger) structures are believed to be related to the polymerized reactive mesogen.

The heights of those structures are better measured by using an Atomic Force Microscope (model Veeco diDimension V). The corresponding results are shown in the Fig. 10. As we can see, the height of well-aligned structures is at the order of 0.2 μm, while the height of chaotic aggregates is significantly larger and may achieve up to 3 μm.

Those microscopy measurements support the electro-optical measurement results by confirming the characteristic sizes of the polymer aggregates, which are in the origin of director non uniformities and corresponding light scattering. Similar experiments (see

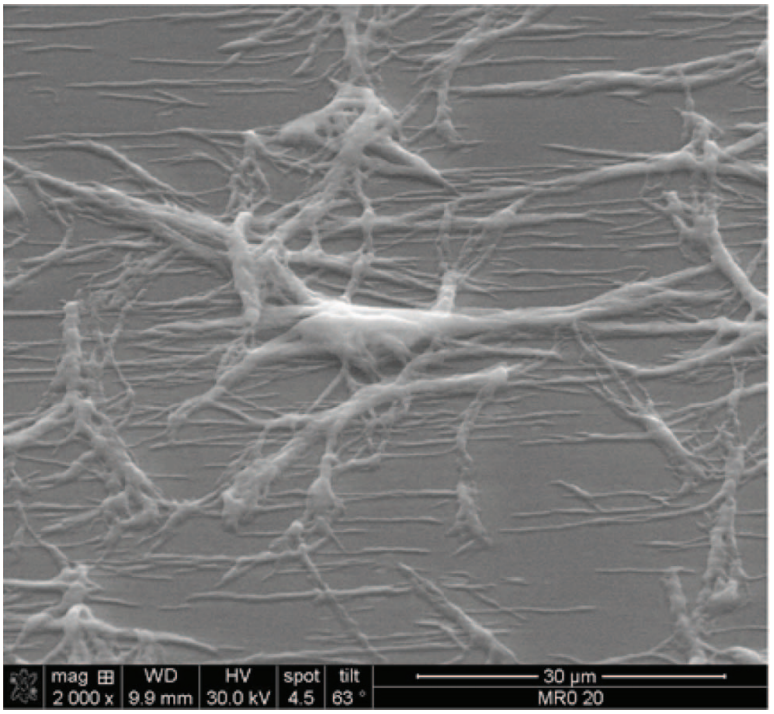

Figure 9. SEM picture of the washed substrate obtained from the S-PSLC cell used in electro-optical measurements.

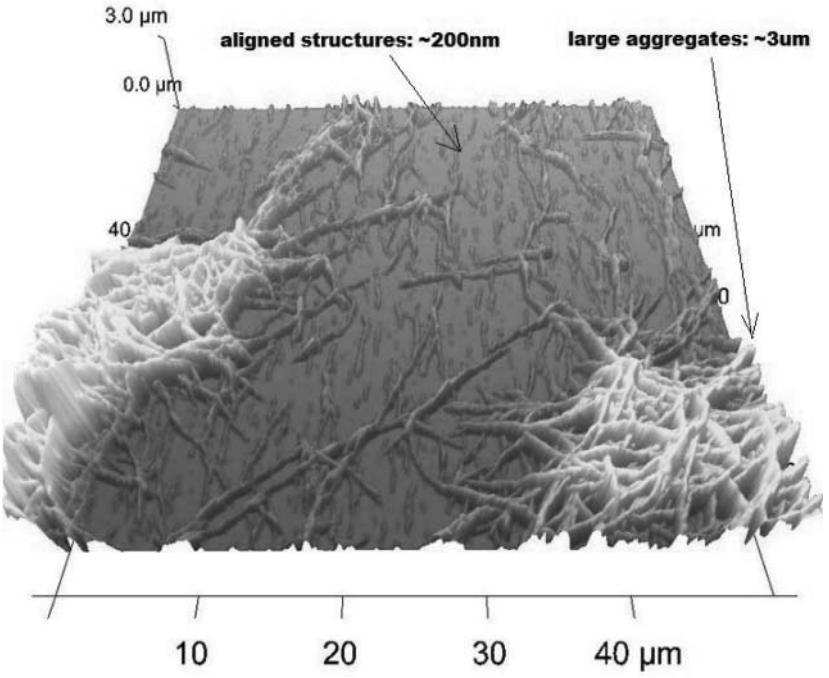

Figure 10. AFM picture of the same substrate used in the Fig. 9.

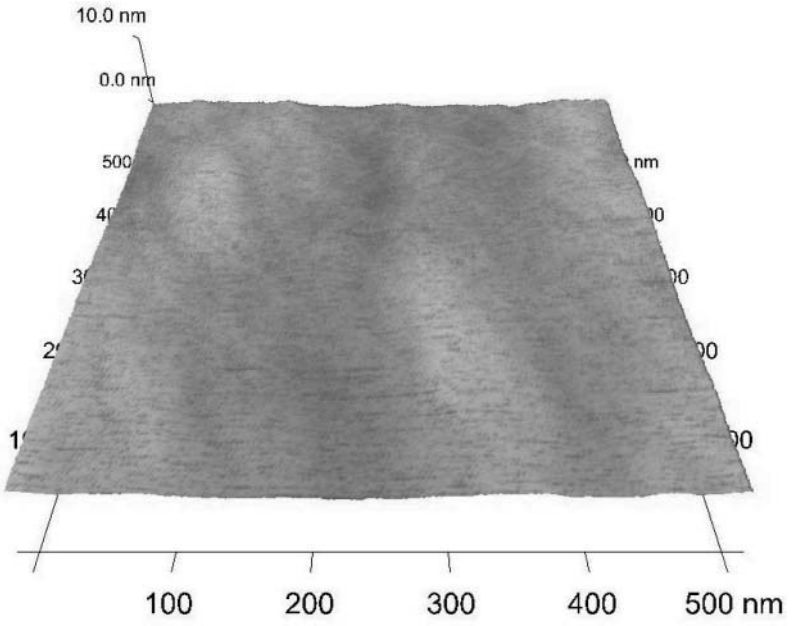

Figure 11. AFM picture of 100% cured RM layer.

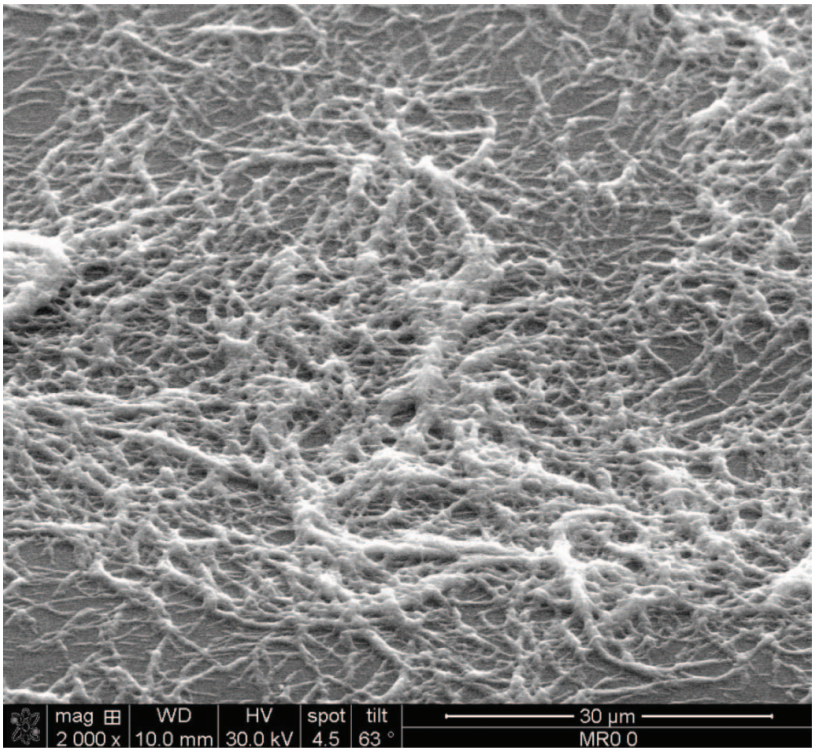

Figure 12. SEM picture of 0% cured RM that was put in contact with non-reactive LC and cured with U = 0 V field.

Fig. 11), performed with fully polymerized RM layers (before their contact with the non-reactive LC) show very smooth surfaces without small or large polymer aggregates described above. The obtained cells have typical (for ordinary, aligned cells) behavior and they are not scattering as the S-PSLCs do.

In contrast, the large aggregates become dominant when the RM is put in contact with the non-reactive LC without a prior partial gelification and without application of an electric field during the UV curing (see an example in the Fig. 12).

Resume and Conclusions

Resuming, thin films of pre-cured RM were cast on rubbed PI-150 surfaces to be used as substrates for LC cells containing pure non-reactive LCs. Their short contact with LC molecules allowed a partial inter-diffusion, which was then slowed down (and ended) by the UV exposition and polymerization of the RM. The application of an electric field (or magnetic field, not discussed here) during the inter-diffusion and UV curing process influenced noticeably the formation of S-PSLC morphology. Electro-optic properties as well as additional microscopic studies brought interesting insight to better understand the obtained structures.

We believe that the described material systems are very promising. They are extremely rich both from scientific and practical points of views. The scientific aspect is first related to the molecular diffusion processes, which are anisotropic and take place in the presence of aligning fields [16,17]. Their practical promise is also very important since they could enable various control parameters (such as pre-curing, contact time, field strength, curing speed, etc.) to influence the final morphology and electro-optical properties of the final cells. This being said, we understand that the polarization dependence of the reported system is a key drawback (particularly for polarizer-free applications). However, the work continues to better understand and better control both material parameters as well as process steps involved to "program" those S-PSLC systems according to our needs. In fact, we have recently shown that, by the appropriate choice of parameters, one can achieve rather good polarization independence (less than 5% of difference between ordinary and extraordinary input probe polarizations) and the corresponding results will be submitted for publication soon.

Acknowledgment

We thank the financial support of Canadian Institute for Photonic Innovations (CIPI), Fonds Québécois de la Recherche sur la Nature et les Technologies (FQRNT) and Natural Sciences and Engineering Research Council of Canada (NSERC).

References

[1] Doane, J. W., Golemme, A., West, J. L., Whitehead, J. B. Jr., & Wu, B.-G. (1988). Polymer dispersed liquid crystals for display application. *Molecular Crystals and Liquid Crystals Incorporating Nonlinear Optics*, *165*(1), 511–532.

[2] (a) Lovinger, A. J., Amundson, K. R., & Davis, D. D. (1994). Morphological investigation of UV-curable polymer-dispersed liquid-crystal (PDLC) materials. *Chem. Mater.*, *6*, 1726–1736; (b) Bouteiller, L., & Le Barny, P. (1996). Polymer-dispersed liquid crystals: Preparation, operation and application. *Liquid Crystals*, *21*(2), 157–174.

[3] Crawford, G. P., & Zumer, S. (Eds.) (1996). *Liquid Crystals in Complex Geometries*, Taylor & Francis: London.

[4] Hikmet, R. A. (1990). Electrically induced light scattering from anisotropic gels. *Journal of Appl. Phys.*, *68*(9), 4406–4412.
[5] Crawford, G. P., Scharkowski, A., Fung, Y. K., & Doane, J. W. (1995). Internal surface, orientational order, and distribution of a polymer network in a liquid crystal matrix. *Phys. Rev. E 52*, R1273.
[6] Choi Sang-Woong, Jo Soo In, Lee You-Jin, Kim Young-Ki, Yoon A Ra, Kim Jae-Hoon, *Pretilt Angle Control of the Liquid Crystal by using the Reactive Mesogen*, http://ddlab.hanyang.ac.kr/inner_image/publication/proceeding/184.pdf.
[7] Furue, H., Iimure, Y., Hasebe, H., Takatsu, H., & Kobayashi, S. (1998). The effect of polymer stabilization on the alignment structure of surface-stabilized ferroelectric liquid crystals. *Molecular crystals and liquid crystals science and technology. Section A, Molecular crystals and liquid crystals*, *317*, 259–271.
[8] Snively, C., Chen, P. Y., Palmer, R. A., & Koenig, J. L. (1996). Stabilization of polymer dispersed liquid crystal systems using surface active agents. *Molecular Crystals and Liquid Crystals Science and Technology. Section A. Molecular Crystals and Liquid Crystals*, *289*(1), 11–23.
[9] Bédard-Arcand, J.-P., & Galstian, T. (2011). Self organization of liquid-crystal and reactive-mesogen into 2d surface stabilized structures. *Macromolecules*, *44*, 344–348.
[10] Merck Product Specifications. http://www.merck-chemicals.com/lcd-emerging-technologies.
[11] de Gennes, P. G., & Prost, J. (1995). *The Physics of Liquid Crystals*, Oxford University Press, 2nd Edition.
[12] Blinov, L. M., & Chigrinov, V. G. (1994). *Electrooptic Effects in Liquid Crystal Materials*, Springer.
[13] (a) Pane, S., Caporusso, M., Ruggieri, S., & Tasselli, F. (1999). Liquid crystal properties modulation for high performance PDLC films. *Molecular Crystals and Liquid Crystals Science and Technology. Section A. Molecular Crystals and Liquid Crystals*, *336*(1), 133–144; (b) Chidichimo, G., De Filpo, G., Manfredi, S., Mormile, S., Tortora, L., Gallucci, C., & Cassano, R. (2009). High contrast reverse mode PDLC films: A morphologic and electro-optical analysis. *Molecular Crystals and Liquid Crystals*, *500*(1), 10–22.
[14] L. Zohrabyan, A.-M. Albu, A. Zohrabyan, & T. Galstian (2010). Light induced gradient polymer stabilized liquid crystals for electrically variable focus lenses: the role of network morphology. *Proc. SPIE*, *7716*, 77160D; doi:10.1117/12.859079.
[15] Nie, X., Lu, R., Xianyu, H., Wu, T. X., & Wu, S.-T. (2007) Anchoring energy and cell gap effects on liquid crystal response time. *J. Appl. Phys.*, *101*, 103110-1–103110-5.
[16] Chien, L.-C., Boyden Mary, N., Walz Andrew, J., Shenouda Ibrahim, G., & Citano Carla M. (1998). Photopolymerization in self-organizing systems. *Molecular Crystals and Liquid Crystals Science and Technology. Section A. Molecular Crystals and Liquid Crystals*, *317*(1), 273–285.
[17] Saad, B., Denariez-Roberge, M. M., & Galstyan, T. (1998) Diffusion of photoexcited azo dyes in liquid crystal host. *Optics Letters*., *23*(9), 727–729.